

# Energetic solar particle dropouts detected by Ulysses at 1.63 AU: A possible encounter with the Earth's distant magnetotail

Stephen M. Ashford, Kinsey A. Anderson, Robert P. Lin, and Jeneen R. Sommers<sup>1</sup>  
Space Sciences Laboratory, University of California, Berkeley

John L. Phillips<sup>2</sup>  
NASA Johnson Space Center, Houston, Texas

**Abstract.** Fast solar particles are used to trace the topology of the interplanetary magnetic field during a solar event detected by the heliosphere instrument for spectra composition and anisotropy at low energy (HISCAL) on the Ulysses spacecraft on January 2, 1991. Two sharp-edged dropouts, lasting for 10 and 25 min, were detected in the fluxes of solar ions from ~130 keV to >1.8 MeV and halo (heat flux) electrons from 71-461 eV, while simultaneously the flux of high-energy, 38-315 keV solar electrons and 56-78 keV ions remained constant. The halo electrons and 130 keV to >1.8 MeV solar ions are traveling with similar speeds,  $\sim 4 \times 10^6$  to  $3 \times 10^7$  m/s, much slower than the energetic solar electrons ( $>10^8$  m/s), and faster than the 56-78 keV ions, suggesting that the dropout field lines were first disconnected from the Sun and then reconnected, with the distance to the reconnection point and time of the reconnection such that >38 keV electrons had already repopulated the dropout field lines. At the time Ulysses was 0.63 AU from the Earth on its way to Jupiter,  $\sim 2^\circ$  above the ecliptic with a Sun-Earth-spacecraft angle of  $\sim 172.8^\circ$ , approximately where the Earth's magnetotail would be expected to be if it extended to 15,000 Earth radii. We consider the possibility that Ulysses encountered interplanetary field lines connected to the magnetotail.

## 1. Introduction

The large-scale topology of interplanetary magnetic field (IMF) lines can be traced on various spatial scales with fast charged particles [see, e.g., Anderson and Lin, 1966; Lin and Anderson, 1966; Krimigis et al., 1967]. The presence of the solar wind halo [Feldman et al., 1975] consisting of electrons escaping from the hot  $\sim 10^6$  K solar corona and carrying heat flux away from the Sun, generally indicates direct magnetic connection to the solar corona. McComas et al. [1989] used brief disappearances of the halo electron population (called heat flux dropouts or HFDs) to identify regimes magnetically disconnected from the Sun, and suggested that HFDs were evidence for magnetic reconnection near the Sun. In addition, the Sun also emits impulsive bursts of more energetic electrons ranging from below  $\sim 1$  keV up to energies of 100s of keV [Anderson and Lin, 1966; Lin, 1985; Lin et al., 1996; Buttigieg et al., 1995] and ions from tens of keV to several MeV [McCracken and Ness, 1966; Anderson and Dougherty, 1986].

In this paper we use halo electrons, and energetic electrons and ions, with a wide range of speeds, to study the dynamics of changing IMF topology during a solar event detected by the Ulysses spacecraft on January 3, 1991. In particular, we will

analyze two sharp dropouts of the halo electrons and energetic ions in which the fast electron flux remained unchanged. The timing of these features suggests the presence of a magnetic reconnection region between the particle source and the spacecraft and place limits on the spatial and temporal scales involved. We will discuss the possibility that the reconnection was caused by an interaction with the Earth's magnetotail. At the time of the particle dropouts, Ulysses was 5 times farther away from the Earth than the most distant encounter with the geotail yet recorded, at  $\sim 3100 R_E$  [Ness et al., 1967; Wolfe et al., 1967; Fairfield, 1968; Intriligator et al., 1969, 1979; Walker et al., 1975].

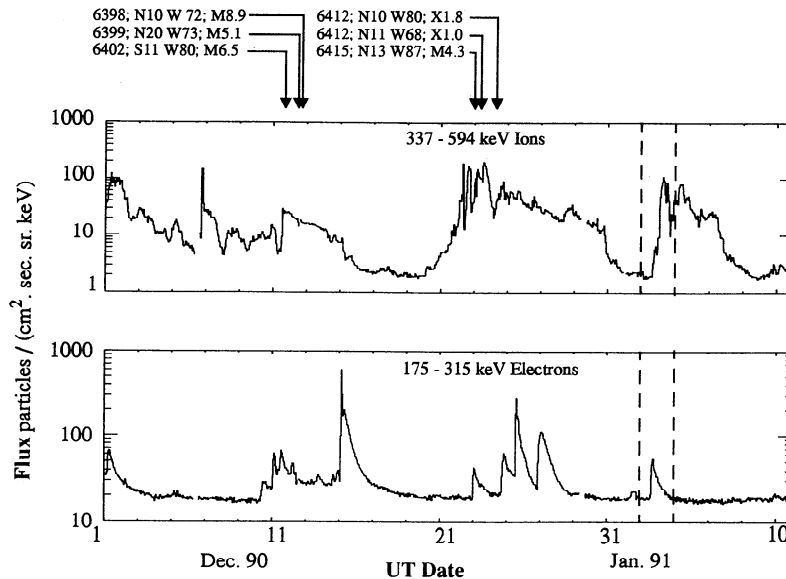
## 2. Event Description

Figure 1 shows one month of ion and electron data taken by the heliosphere instrument for spectra composition and anisotropy at low energy (HISCAL) on Ulysses containing the event (shown between dashed lines) discussed in this paper. A solar active region magnetically connected to Ulysses at the time would have been located near the western limb of the Sun. GOES X ray observations of large flares emanating from that region are shown on the plot. There were no large X ray events observed between January 1 and 3, suggesting that the active region that was the source of this event had passed over the western limb and was not visible. The relative configuration of the Earth, Sun, and Ulysses at the time of the event is shown in Figure 2.

The solar energetic particle event of interest is shown in detail in Figure 3. The event can be broadly divided into three phases. The first lasted from about 1000 to 1430 UT on January 2 and saw a rise in the ion flux by about a factor of 10 in the highest two energy channels only (1070-4750 keV). In the second phase,

<sup>1</sup>Now at the Hansen Experimental Physics Laboratory, Stanford University, Palo Alto, California.

<sup>2</sup>Also at Los Alamos National Laboratory, Los Alamos, New Mexico.



**Figure 1.** A plot of high-energy ions and electrons recorded by the HISCALE instrument on board Ulysses over a complete solar rotation. The event discussed in this paper is shown by the dashed lines (the ion dropouts are not visible at the time resolution of this plot). Note that there is no event seen 26 days (one solar rotation) before the January 2 event. The arrows show the times of GOES X ray observations for large solar flares occurring near the western limb of the Sun, annotated in the format NOAA/USAF region; latitude and central meridional distance (CMD); X ray importance.

~1430 UT January 2 to ~0100 UT January 3, the ion fluxes increased in the four highest channels (340-4750 keV). The third phase began at about 0100 on January 3 when all energy channels (except the two lowest, 56-130 keV) simultaneously saw the ion flux ramp up over about an hour, by about a factor of 10. The 78-130 keV channel showed an abrupt increase at ~0200 UT on January 3, while the lowest energy (56-78 keV) channel began a slow increase at ~0400 UT. The ion fluxes show broad, relatively flat, peaks, dispersed in energy with the highest channel peaking at ~0400 UT down to the lowest, which peaked at ~0800 UT.

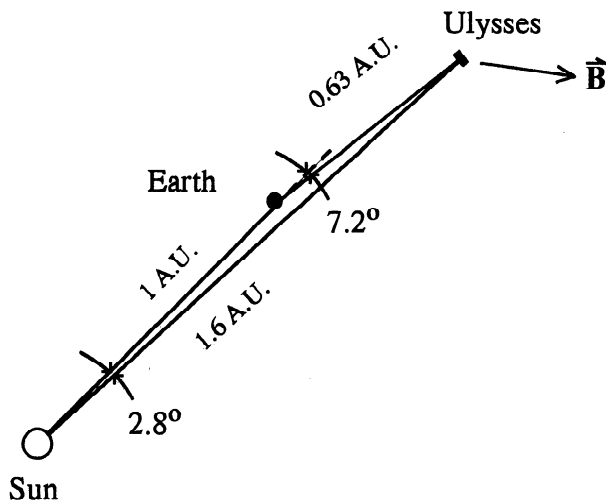


**Figure 2.** At the time of the event discussed in this paper, Ulysses was  $\sim 2^\circ$  above the ecliptic plane 0.63 AU from the Earth. The Sun-Earth-spacecraft angle was  $172.8^\circ$ . During the event the interplanetary magnetic field was broadly in the spiral field direction as indicated.

These broad maxima lasted for at least several hours before gradually decaying. The ion observations therefore are consistent with an impulsive solar energetic ion event, showing velocity dispersion, with superimposed spatial features.

At about 1500 UT on January 2 a field-aligned electron flux was detected with a very rapid onset and no observable velocity dispersion. The electron flux increased rapidly in all energy channels to a maximum at about 1900 UT on January 2, and then slowly decayed over the first half of the following day. The electrons also appear to have originated from an impulsive event, but the lack of dispersion indicates that Ulysses did not observe the temporal onset, but rather moved onto field lines already populated by electrons.

On two occasions, 0930-0945 and 1030-1100 UT on January 3 the ion flux fell sharply back to the levels before the rapid rise at 0100 on January 3. These dropouts were most apparent in the energy range above  $\sim 130$  keV up to the detector's maximum energy range of 4.75 MeV. Note that the dropouts were not seen in the lowest ion energy channel (56-78 keV) and possibly not in the second channel (78-130 keV). At the time of these ion dropouts, the 38-315 keV solar electrons (Figure 3, top) as measured by the Wart B electron detector in low-energy magnetic spectrometer (LEMS) 30 showed no change in flux (see the appendix for details of the instruments used in this study).

The dropouts are shown in more detail in Figure 4. Figure 4 (bottom) contains data from the Los Alamos solar wind observations over the poles of the Sun (SWOOPS) detector on Ulysses, showing the HFDs in the halo electrons at all energies simultaneously with the fast ion dropouts. Note that these halo electrons have much lower energies ( $\sim 0.1$  keV) than the electrons detected by Wart B. The SWOOPS detector produces a halo electron spectrum approximately every 5 min, and to within this temporal resolution the halo dropouts and the ion dropouts coincided in time.

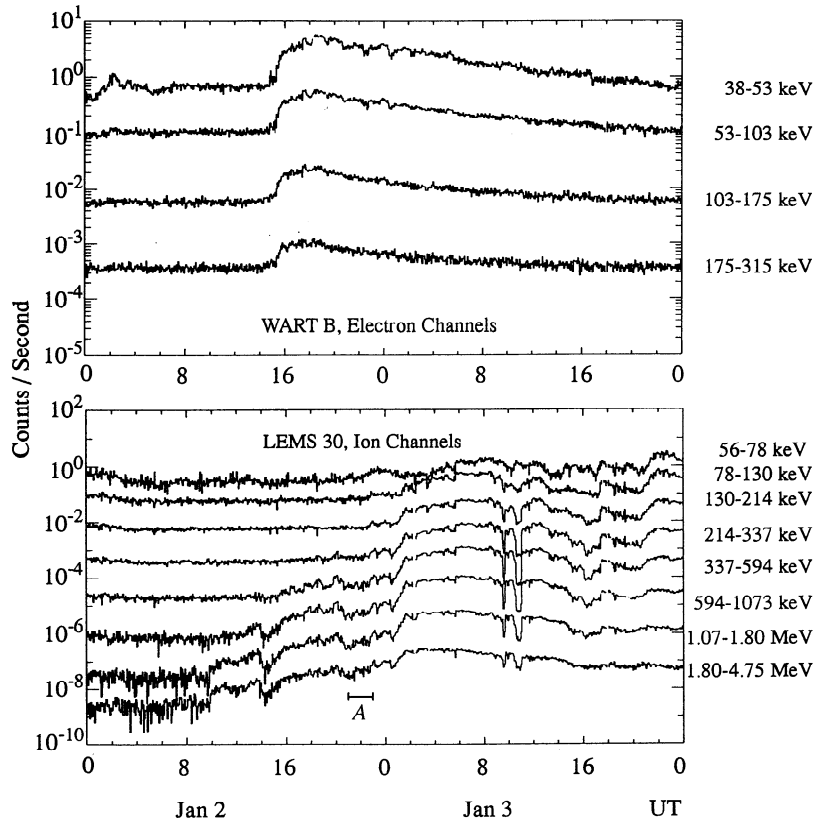


**Figure 3.** (top) Spin-averaged count rates recorded by the Wart B electron detector and (bottom) data from the LEMS 30 ion detector. The two ion dropouts are clearly visible at around 1000 UT on January 3. The point marked A corresponds to the spectra and pitch angle distributions shown in Figures 5 and 6. The times corresponding to points B through F are shown in Figure 4. Note that the fast electron flux shows no dropouts. Note also that no dropouts are observed in the flux of ions in the lowest two energy channels (56-130 keV), although the flux in this channel is above background.

There is a possible third dropout at around 1600 UT on January 3. At this time there was an HFD in the halo electrons, but the ion drop is not very clearly defined. By this stage of the event the electron flux had fallen to near the Wart B detector's background level, so this dropout cannot be compared to the first two. This analysis will focus on the first two ion dropouts.

During the events discussed, the IMF was broadly in the direction expected for a Parker spiral, with a fairly constant magnitude of  $\sim 7$  nT (data from the magnetometer on board Ulysses, A. Balogh, Principal Investigator). There was a sharp decrease in the component normal to the ecliptic, from  $\sim 2$  nT to  $\sim 4$  nT coincident with the onset of the first dropout, and the normal component rose to  $\sim 2$  nT at the end of the first dropout, but there were no obvious changes in the magnetic field during the second dropout. There were no discontinuities in the solar wind during the events. The solar wind speed on January 3 started at 370 km/s and decreased steadily to  $\sim 340$  km/s over the day, and the ion density was steady at  $\sim 3$  cm $^{-3}$ . The alpha particle abundance is steady at about 9%. The solar wind flow was directed about  $5^\circ$  south from the start of the day until 0810 UT when it ramped up to zero polar angle at about the time of the dropouts, then it slowly declined again.

Spectra and pitch angle distributions (PADs) were calculated for six intervals marked A through F in Figures 3 and 4. The ion spectra are shown in Figure 5, the ion PADs are shown in Figure 6, and the electron PADs are shown in Figure 7. During

the intervals B, D, and F, the ion spectra have a distribution peaked at around 100 keV and the PADs are strongly field aligned, flowing away from the Sun. The spectra and PADs in C and E are markedly different. The spectra show no peak, and the PADs are flat, indicating an approximately isotropic flux (although at these times the fluxes were too low to calculate accurate PADs). Thus it appears that intervals in C and E comprise one regime and B, D, and F comprise another. During the interval A, the ion flux was similar to that in C and E, and the spectrum was similar except that the spectrum for A shows a turnover at the very lowest (56-78 keV) energy channel. The ion PAD at A, however, is distinctly different from C and E, in that it shows a field aligned anisotropy. A may represent the same regime as C and E but at an earlier stage in its evolution.

In contrast, the fast electron PADs, constructed with the low-energy foil spectrometer (LEFS) electron telescope observations (the Wart B telescope does not have enough angular coverage to produce PADs), show outward flowing fluxes throughout the dropout region (see Figure 7). It appears that the PADs are more sharply peaked during times when there is a high ion flux than during the dropouts. Analysis shows that the differences between the PADs during and outside the dropouts is entirely due to contamination of the LEFS electron telescope by ions with sufficient energy to penetrate the foil (see the appendix) and that to within experimental uncertainty, the electron fluxes and angular distributions are constant throughout the dropouts. The

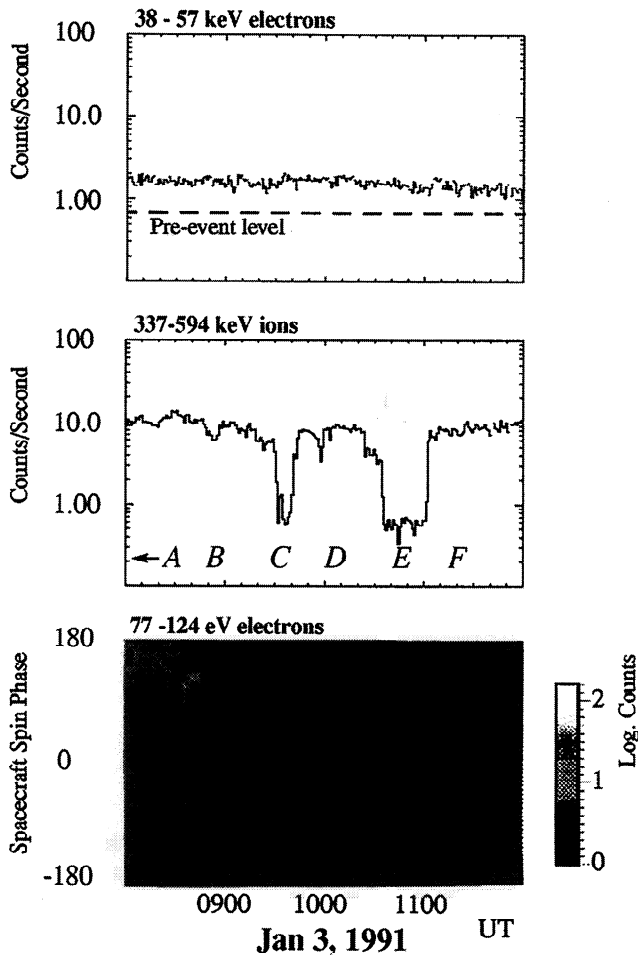


**Figure 4.** (top) Spin-averaged flux rates recorded by the Wart B electron detector and (middle) data from the LEMS30 ion detector. (bottom) The halo electrons observed by the Los Alamos SWOOPS detector as intensity, shown by the grey scale, plotted against the spacecraft spin phase. The dropouts in the solar ions are clearly visible, as is the absence of any change in the flux of fast electrons. The halo electrons dropout at all angles simultaneously with the ions. The five points marked B through F correspond to the spectra and PADs discussed later. Point A appears in Figure 3.

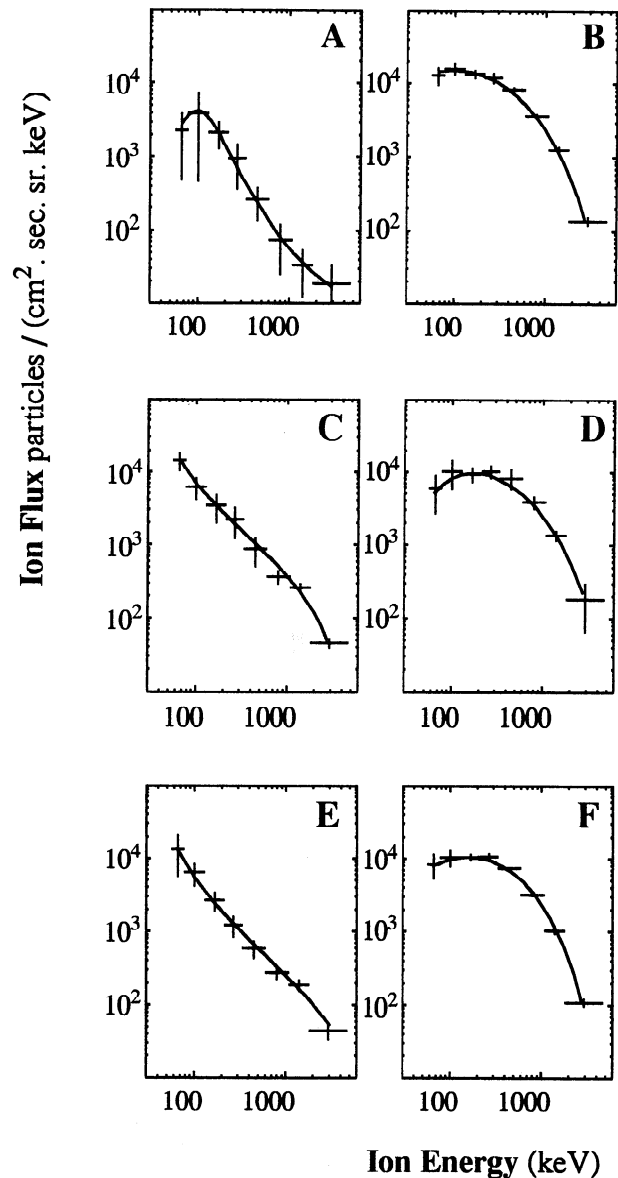
true electron PAD is that shown in Figure 7c or 7e during the ion dropouts when there was very little ion contamination. This picture is reinforced by the fact that the electron flux observed by Wart B (which is not subject to ion contamination) does not show dropouts (see Figure 4). Data points from the uncontaminated Wart B have been added, where possible, to Figure 7 to show that the true PADs are the same inside and outside the dropouts.

### 3. Discussion

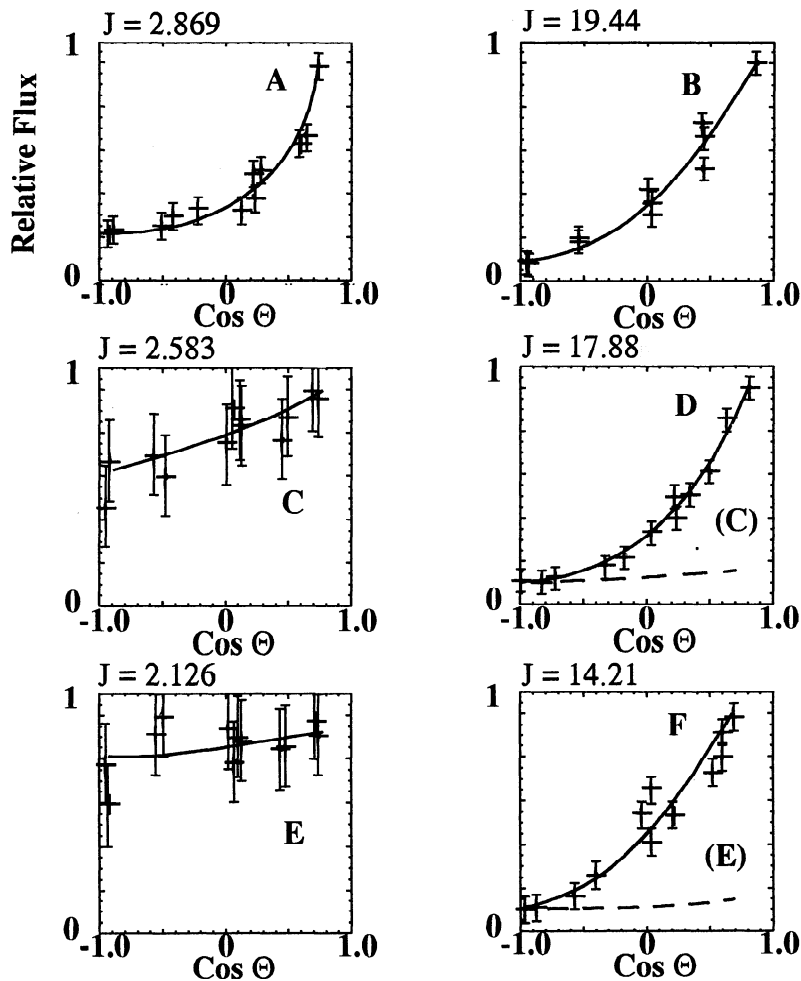
The lack of velocity dispersion implies that the dropouts in the data represent spatial structures convecting past the spacecraft. On January 3 the solar wind speed started at about 370 km/s and decreased steadily to about 340 km/s at the end of the day. Taking into account the magnetic field direction during the event, the widths of the two dropout regions are estimated to be  $\sim 2 \times 10^5$  and  $\sim 5 \times 10^5$  km.

Table 1 below shows the energies, velocities (for  $0^\circ$  pitch angle particles) and times to travel 1 AU, for the halo electrons, fast electrons, 0.078-4.75 MeV ions, and 56-78 keV ions. Note that the halo electrons and fast ions cover roughly the same velocity range, whereas the fast electrons are much faster ( $\sim 0.3-0.7 c$ ), and the 56-78 keV ions are slower.

The HFDs indicate intermittent magnetic disconnection. Consider a field topology, shown in Figure 8, with two types of field line, those connected directly back to the Sun (labeled I), and those (II) which have recently disconnected from, and then



**Figure 5.** These spectra from the LEMS 30 telescope were taken at six times during the event labeled A through F in Figure 4. (a) the spectrum at 1500 on January 2, at the onset of the event. (b), (d), and (f) The spectra during the event at 0900, 1015 and 1110 UT, respectively on January 3 and (c) and (e) are the spectra taken during the two ion and halo electron dropouts at 0933 and 1050 UT. The dropout spectra in Figures 5c and 5e are clearly different from the spectra in Figure 5b, 5d, and 5f. The peak in spectrum in Figure 5a at  $\sim 100$  keV is possible evidence of velocity dispersion at the onset of the ion event.



**Figure 6.** Ion pitch angle distributions for the energy range 1.07 - 1.80 MeV for the six times identified in Figure 4 during the event. In each panel the flux is normalized to the highest point and plotted against  $\cos$  pitch angle. The flux level each plot is normalized to is shown above the top left of each panel in units of particles / (cm<sup>2</sup> s sr keV). Figures 6c and 6e show a nearly isotropic flux during the dropouts compared with a strongly field aligned anisotropy at times in A, B, D, and F. For comparison, the PADs for C and E are overlaid as dashed lines on the plots for D and F.

reconnected to the Sun. While the type II lines were disconnected, they are cut off from the source of solar particles, so they soon become depopulated of fast solar electrons and ions and halo electrons. When the type II lines are reconnected to the Sun, they are rapidly repopulated by the fast electrons within tens of minutes, but the halo and fast ions take hours to refill the lines. When the solar energetic particles were first encountered at A, Ulysses was on a type I field line. Presumably, the rise in flux at ~0100 UT on January 3 was due to the spacecraft crossing onto field lines, still type I, but connected to a different part of the solar source region. This explanation is illustrated schematically in Figure 9. Thus we identify the times A, B, D, and F with type I field lines and the dropouts C and E with type II field lines. The ion distributions seen during C and E have similar flux levels and spectra to those observed in A, suggesting that these may be ions from early in the solar event that have streamed into the outer heliosphere beyond Ulysses, where they were backscattered, possibly by inhomogeneities in the outer heliospheric magnetic field. These backscattered ions then traveled inward, back past Ulysses, and were mirrored by the stronger field inside Ulysses' orbit to form the nearly isotropic PAD. The interval between A

and C, and the speed of the ions (see Table 1) suggest that the backscattering region was within ~0.5 AU of Ulysses.

Assume that the site of disconnection and reconnection occurs a distance  $L$  away from Ulysses along the field line. Then the travel time from the site to Ulysses is  $\Delta t = L / v_i$  for particle  $i$  with speed  $v$  along the field. Since the fast electrons do not show a dropout, the reconnection must have happened  $\Delta t_r > L / v_{fe}$  beforehand, where  $v_{fe}$  is the fast electron speed. Because the halo electrons and fast ions do show the dropouts, the reconnection must have happened at  $\Delta t_r < L / v_{fi,ho}$ , where  $v_{fi,ho}$  is the fast ion or halo electron speed. The lowest energy channel ions flux does not show a dropout, whereas the third and higher energy channels do, which implies that the disconnection occurred between  $L / v_{fi} < \Delta t_d < L / v_{fi}$ . The location of Ulysses at this time (Figure 2) suggests the possibility that the field lines may be connected to the Earth's magnetotail. If the disconnection and reconnection occurred near the Earth, we have  $L \sim 0.7$  AU, and then  $16 \text{ min} < \Delta t_r < 1.6$  hours, and  $6 < \Delta t_d < 8$  hours. If the disconnection and reconnection site was near the Sun,  $L \sim 2-3$  AU and  $50-65 \text{ min} < \Delta t_r < 5-6.5$  hours and  $17 < \Delta t_d < 34$  hours. The observations are consistent with both possibilities.

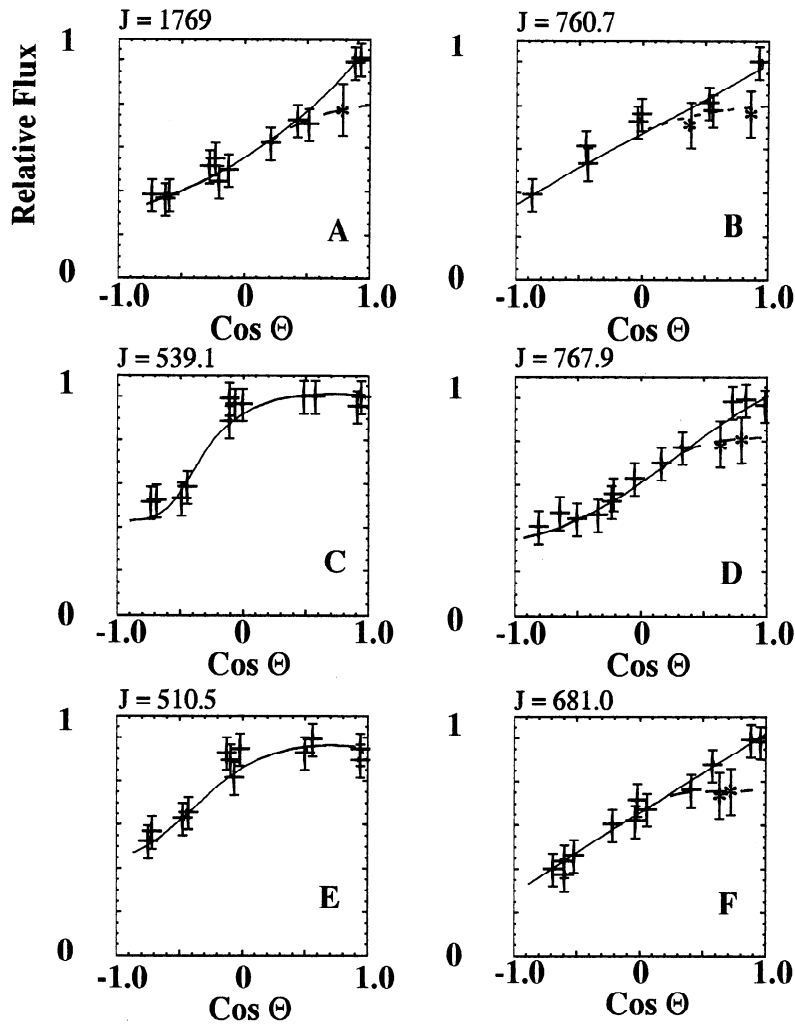


**Figure 7.** Electron pitch angle distributions for the energy range 40–64 keV for the same six time intervals as the ion PADs in Figure 6. In each panel the flux is normalized to the highest point and plotted against  $\cos$  pitch angle. The flux level each plot is normalized to is shown above the top left of each panel in units of particles / ( $\text{cm}^2 \text{ s sr keV}$ ). In contrast to the ion PADs the electron PADs show a field-aligned anisotropy throughout the event. The solid lines in the plots show the measured fluxes, and the dashed lines in Figures 7a, 7b, 7d, and 7f show the calculated fluxes with ion contamination removed, (the ion flux was very low in Figures 7c and 7e). The data points in Figures 7a, 7b, 7d, and 7f marked with a star are from the Wart B detector. There was no significant change in the electron PADs during the ion dropouts.

At the observed speed of 340–370 km/s, the solar wind covers the distance from the Earth to Ulysses in around 3 days. Thus for the geomagnetic tail to be connected to the Earth and extend out to Ulysses ( $\sim 15,000 R_E$ ), magnetic reconnection across the tail must stop for about this long. Lunar shadowing observations of the convection speed of magnetic field lines which are connected at one end to the Earth and at the other end to the IMF [McCoy *et al.*, 1975] indicate that this is highly unlikely. Typically, the

Earth-connected tail field lines only extend to  $\sim 10^3 R_E$  behind the Earth before they reconnect across the tail.

However, magnetic loops (islands) may be formed in the tail reconnection process [Hesse and Birn, 1991]. These loops will be convected antisunward from the Earth. Since the loops have been disconnected from the Sun, they have presumably been depopulated of solar particles. Assume such a loop of path length  $L$  reconnects into a heliospheric field line at a distance  $l$  from Ulysses. Ulysses then encounters the field line a time  $\Delta t_r$  after the reconnection. The time and distance constraints are now  $\Delta t_r > (L + l) / v_{fe}$  since the fast electrons have already reached Ulysses;  $\Delta t_r < (L + l) / v_{f,he}$ , as the halo electrons and fast ions have not; and  $l / v_{fi} < \Delta t_r < l / v_{li}$ , since the lowest energy ions (56–78 keV) have not yet depopulated the field line in the vicinity of Ulysses, whereas the  $>130$  keV ions have.

After the reconnection, the fastest ions (1.8–4.75 MeV) from just upstream of the reconnection point would cover the extra distance  $L$  and catch up with the halo electrons and  $\sim 130$  keV

**Table 1.** Typical Velocities of Solar Particles

|   | Velocity ( $\alpha = 0^\circ$ ),<br>m/s           | Time to Travel<br>1 AU, hours |
|---|---|-------------------------------|
| 77 - 124 eV halo electrons                      | $v_{he} = 5.2 - 6.6 \times 10^6$                  | 6 - 8                         |
| 38 - 315 keV fast electrons                     | $v_{fe} = 1.1 - 2.4 \times 10^8$                  | 0.17 - 0.38                   |
| 130 keV - 4.75 MeV fast ions<br>(with dropouts) | $v_{fi} = 5.0 \times 10^6$<br>$- 3.0 \times 10^7$ | 1.5 - 8.3                     |
| 56 - 78 keV fast ions<br>(without dropouts)     | $v_{li} = 3.3 - 3.9 \times 10^6$                  | 10 - 13                       |

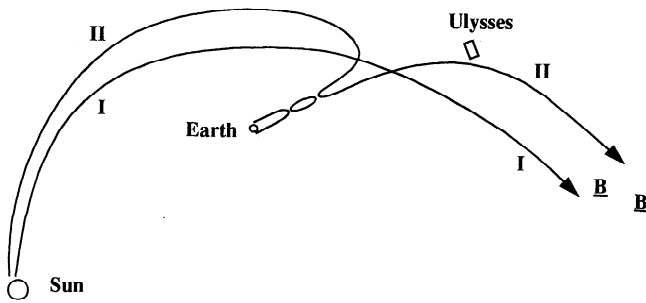


**Figure 8.** An encounter with the Earth's deep geomagnetic tail could involve meeting regions with different magnetic connection. The field line labeled I is directly connected to the Sun and is populated by fast ions and halo electrons. The type II line has been intermittently reconnected into the Earth's magnetotail. At the time of the encounter it has been repopulated by fast electrons but not by the slower halo electrons and 78 keV to 4.75 MeV ions. The even slower 56-78 keV ions have not yet depopulated the field line. The reconnection process in the magnetotail is thought to create magnetic loops as illustrated here.

ions from just downstream of the reconnection point, narrowing the interval in which an HFD and fast ion dropout could be observed simultaneously. Hence the maximum duration of dropout that could be observed by a spacecraft encountering those field lines is determined by the size of the loop and the distance from the reconnection point to the spacecraft. The lower limit to  $L$  and the upper limit to  $l$  are given by  $l/v_{he} = (l + L)/v_{fi} - T_d$ , where  $T_d$  is the duration of the dropout that needs to be accommodated. Since the largest dropout lasted for ~25 min, a small value of  $l$ , say  $l \sim 100 R_E$ , places a lower limit on the size of the loop of  $L \sim 4600 R_E$ . A single loop of this size would be  $2300 R_E$  long; this is longer than typical tail lengths, but not outside the range of observed convection distances [McCoy *et al.*, 1975]. The reconnection process in the magnetotail occurs in three dimensions and may well form structures with multiple loops, as illustrated in Figure 10.

Studies have indicated that energetic particles can propagate in well-defined magnetic channels, [see Anderson and Dougherty, 1986; Buttighoffer *et al.*, 1995]. The types I and II field lines discussed above could represent two different propagation channels of this type. Buttighoffer *et al.*'s [1995] study suggests

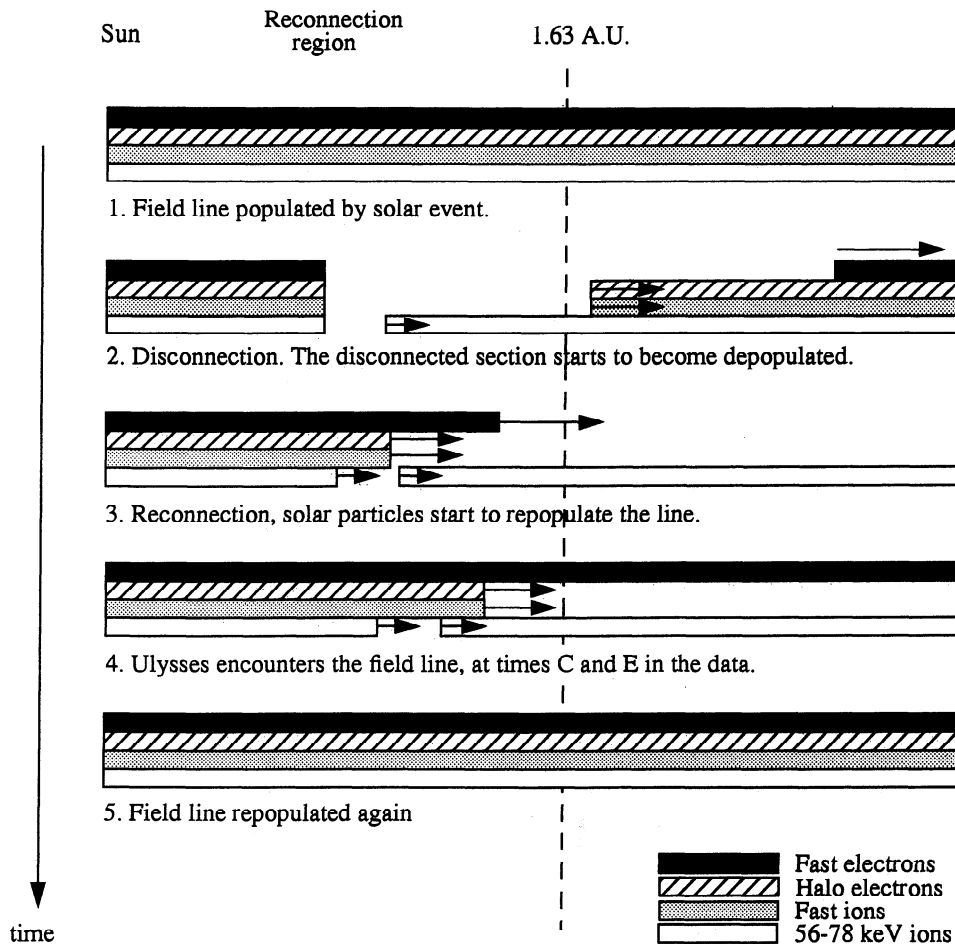


**Figure 9.** A schematic illustration showing the populations of the four types of particle discussed on a type II field line at five times during the event. The field line has been straightened out for clarity. At the time Ulysses encounters the field line in C and E, it has been repopulated by fast electrons, and the slower ions are still there, but the halo electrons and fast ions have not yet repopulated the field line, shown here at stage 4. Hence the observed dropouts. The states of the type II field line shown at stages 1, 2, 3 and 5 were not observed since during these times Ulysses was connected to type I field lines. The speeds are not shown to scale, for the timing analysis, see the text.

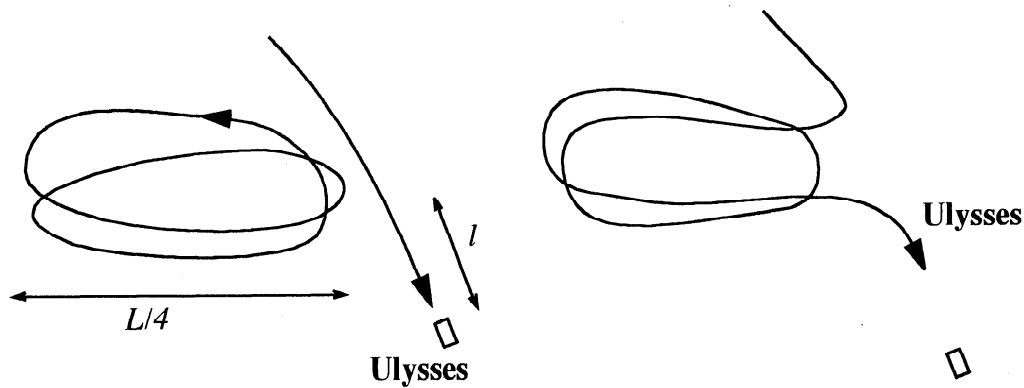


**Figure 10.** A magnetic loop, containing no solar particles, reconnecting into a solar field line at a point  $l$  from Ulysses, would add an extra path length  $L$ . Fast electrons would rapidly repopulate the field line, the halo electrons and fast ions would take longer, and hence the observed dropouts when Ulysses encountered the field line.

the likelihood of filamentation and reconnection in the near-Sun solar wind. Such a scenario could give rise to the dropouts observed without the need for the involvement of the Earth's magnetotail. As mentioned earlier, solar wind heat flux dropouts (HFDs) have previously been observed and attributed to disconnections of the IMF from the Sun [McComas *et al.*, 1989]. Lin and Kahler [1992] found simultaneous fast ( $>2$  keV) electron dropouts for two HFDs but no change in the flux of fast electrons for the other 23 HFDs. They concluded that there were only the two instances where the interplanetary field was truly disconnected from the Sun. The HFDs for which the fast electron flux did not show a dropout could be due to a disconnection followed by a reconnection as discussed here. McComas *et al.* and Lin and Kahler discussed other possible explanations for HFDs without fast electron dropouts that do not involve disconnection, such as the presence of regions of increased plasma density near the Sun leading to enhanced Coulomb scattering of the halo electrons, or electric fields which prevent the escape of halo electrons.

The two HFDs analyzed in this paper are, to our knowledge, unique in that they have simultaneous ion dropouts. A systematic search through the Ulysses data has not revealed any other events like this one. Since the Coulomb collision cross section decreases with mass,  $\sigma \sim q^4 / (m^2 v^4)$ , the fast ions with comparable speeds to the halo electrons are much less prone to scattering, and of course, electric fields could not stop both electrons and ions. The fact that this combination of HFDs, and ion dropouts with the fast electron flux constant, has only been observed in this one case, when the spacecraft was in the region downstream of the Earth, where the magnetotail would be expected to be should it extend to that length, is highly suggestive, although we found no features in the solar wind or interplanetary magnetic field to support the hypothesis that Ulysses encountered the magnetotail. The magnetotail appears to maintain a coherent structure out to at least  $1000 R_E$ . [Fairfield, 1968; Walker, *et al.*, 1975], but little is known about its structure beyond that distance. The data presented here suggest that magnetic structures associated with the Earth's magnetotail may extend out as far as  $\sim 0.6$  AU.

### Appendix: Instrument Description

The HISCALE instrument [Lanzerotti *et al.*, 1992] consists of four silicon detector telescopes (SSTs) (see Figure 11). Two of them, LEMS 30 and LEMS 120, are ion detectors with broom

magnets in front of the apertures to sweep away incoming electrons. The electrons that are magnetically swept away from LEMS 30 are swept into a separate detector, Wart B, deep inside the instrument. Wart B has a small geometric factor but has no response to energetic ions and thus provides a pure electron detector. Wart B provides only partial angular coverage and does not measure all pitch angles for most magnetic field orientations; it is therefore not used to compute PADs. The other two telescopes, LEFS 60 and LEFS 150 are electron detectors with thin foils over the apertures to stop incoming ions below  $\sim 300$  keV. The LEFS detectors are subject to contamination by ions with sufficient energy to penetrate the foil ( $> 300$  keV). The spin axis of Ulysses points toward the Earth and as the spacecraft spins the four SSTs sweep out a nearly full  $4\pi$  field of view.

Also on board the Ulysses spacecraft is the Los Alamos SWOOPS detector which gives 3-D velocity space coverage of electrons and ions in the solar wind plasma [Bame *et al.*, 1992]. In this study we have used SWOOPS observations of electrons over an energy range of 77-243 eV.

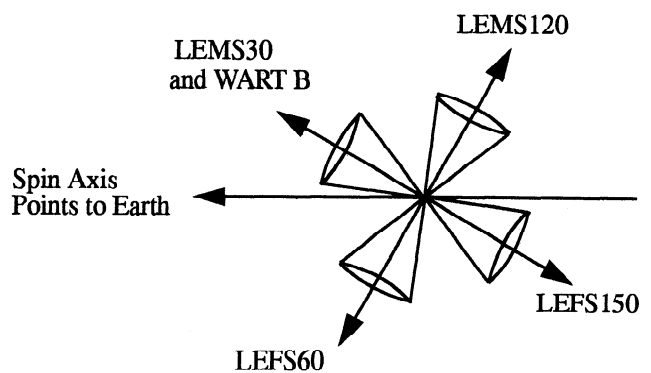


**Figure 11.** The four telescopes are oriented as shown with respect to the spin axis which always points earthward. The angle in degrees between the axis of the field of view and the spacecraft spin axis is designated by the number, e.g., LEMS 30 is at  $30^\circ$  to the spin axis. The LEMS telescopes detect ions and the LEFS measure electrons. The LEMS 30 ion detector and the Wart B electron-only detector point in the same direction. All the detectors have conical fields of view with a full width half maximum (FWHM) of  $45^\circ$ . As the spacecraft spins, the instrument sweeps out a nearly  $4\pi$  field of view.



**Acknowledgments.** The research at the University of California, Berkeley, was supported in part by funding from the National Aeronautics and Space Agency through contract 601012-0, and contract JHU-717043 from the Applied Physics Laboratory of Johns Hopkins University. The work by John L. Phillips was carried out at Los Alamos National Laboratory under the auspices of the U.S. Department of Energy. The editor thanks one referee for his assistance in evaluating this paper.

## References

- Anderson, K. A., and R. P. Lin, Observations on the propagation of solar flare electrons in interplanetary space, *Phys. Rev. Lett.*, **16**, 1121, 1966.
- Anderson, K. A., and W. M. Dougherty, A spatially confined long-lived stream of solar particles, *Sol. Phys.*, **103**, 165, 1986.
- Bame, S. J., D. J. McComas, B. L. Barraclough, J. L. Phillips, K. J. Sofaly, J. C. Chavez, B. E. Goldstein, and R. K. Sakurai, The Ulysses solar wind plasma experiment, *Astron. Astrophys. Suppl. Ser.*, **92**, 237, 1992.
- Buttighoffer, A., M. Pick, E. C. Roelof, S. Hoang, A. Mangeney, L. J. Lanzerotti, R. J. Forsyth, and J. L. Phillips, Coronal electron stream and Langmuir wave detection inside a propagation channel at 4.3 AU, *J. Geophys. Res.*, **100**, 3369, 1995.
- Fairfield, D. H., Simultaneous measurements on three satellites and the observation of the geomagnetic tail at 1000  $R_E$ , *J. Geophys. Res.*, **73**, 6179, 1968.
- Feldman, W. C., J. R. Asbridge, S. J. Bame, M. D. Montgomery, and S. P. Gary, Solar wind electrons, *J. Geophys. Res.*, **80**, 4181, 1975.
- Hesse, M., and J. Birn, Plasmoid evolution in an extended magnetotail, *J. Geophys. Res.*, **96**, 5683, 1991.
- Intriligator, D. S., J. H. Wolfe, D. D. McKibbin, and H. R. Collard, Preliminary comparison of solar wind plasma observations in the geomagnetospheric wake at 1000 and 500 Earth radii, *Planet. Space Sci.*, **17**, 321, 1969.
- Intriligator, D. S., H. R. Collard, J. D. Mihalov, O. L. Vaisberg, and J. H. Wolfe, Evidence for Earth magnetospheric tail associated phenomena at 3100  $R_E$ , *Geophys. Res. Lett.*, **6**, 585, 1979.
- Krimigis, S. M., J. A. Van Allen, and T. P. Armstrong, Simultaneous observations of solar protons inside and outside the magnetosphere, *Phys. Rev. Lett.*, **18**, 1204, 1967.
- Lanzerotti, L. J., R. E. Gold, K. A. Anderson, T. P. Armstrong, R. P. Lin, S. M. Krimigis, M. Pick, E. C. Roelof, E. T. Sarris, G. M. Simnett, and W. E. Frain, Heliosphere instrument for spectra, composition, and anisotropy at low energies, *Astron. Astrophys.*, **92**, 207, 1992.
- Lin, R. P., and K. A. Anderson, Evidence for connection of geomagnetic field lines to the interplanetary field, *J. Geophys. Res.*, **71**, 4213, 1966.
- Lin, R. P., Energetic solar electrons in the interplanetary medium, *Sol. Phys.*, **100**, 537, 1985.
- Lin, R. P., and S. W. Kahler, Interplanetary magnetic field connection to the Sun during electron heat flux dropouts in the solar wind, *J. Geophys. Res.*, **97**, 8203, 1992.
- Lin, R. P., D. Larson, J. McFadden, C. W. Carlson, R. E. Ergun, K. A. Anderson, S. Ashford, M. McCarthy, G. K. Parks, H. Reme, J. M. Bosqued, C. d'Uston, T. R. Sanderson, and K. P. Wenzel, Observations of an impulsive solar electron event extended down to  $\sim 0.5$  keV energy, *Geophys. Res. Lett.*, **23**, 1211, 1996.
- McComas, D. J., J. T. Gosling, J. L. Phillips, S. J. Bame, J. G. Luhmann, and E. J. Smith, Electron heat flux dropouts in the solar wind: evidence for interplanetary magnetic field reconnection?, *J. Geophys. Res.*, **94**, 6907, 1989.
- McCoy, J. E., R. P. Lin, R. E. McGuire, L. M. Chase, and K. A. Anderson, Magnetotail electric fields observed from lunar orbit, *J. Geophys. Res.*, **80**, 3217, 1975.
- McCracken, K. G., and N. F. Ness, The collimation of cosmic rays by the interplanetary magnetic field, *J. Geophys. Res.*, **71**, 3315, 1966.
- Ness, N. F., C. S. Seearce, and S. C. Cantarano, Probable observations of the geomagnetic tail at 103 Earth radii by Pioneer 7, *J. Geophys. Res.*, **72**, 3769, 1967.
- Walker, R. C., U. Villante, and A. J. Lazarus, Pioneer 7 observations of plasma flow and field reversal in the distant geomagnetic tail, *J. Geophys. Res.*, **80**, 1238, 1975.
- Wolfe, J. H., R. W. Silva, D. D. McKibbin, and R. H. Mason, Preliminary observations of a geomagnetospheric wake at 1000 Earth Radii, *J. Geophys. Res.*, **72**, 4577, 1967.

---

S. Ashford, K. A. Anderson, and R. P. Lin, Space Sciences Laboratory, University of California, Berkeley, CA 94720-7450. (e-mail: ashford@ssl.berkeley.edu)  
 J. L. Phillips, NASA Johnson Space Center, Code CB, 2101 NASA Road 1, Houston, TX 77058 (e-mail: jlphilli@ems.jsc.nasa.gov)  
 J. R. Sommers, Hansen Experimental Physics Laboratory, Annex B124, Stanford University, Stanford, CA 94305-4085 (e-mail: jenceen@quake.stanford.edu)

(Received June 6, 1997; revised October 3, 1997; accepted October 7, 1997.)